# Rotenone, Deguelin, Their Metabolites, and the Rat Model of Parkinson's Disease

**ARTICLE** *in* CHEMICAL RESEARCH IN TOXICOLOGY · NOVEMBER 2004

Impact Factor: 3.53 · DOI: 10.1021/tx049867r · Source: PubMed



**7 AUTHORS**, INCLUDING:

Pierluigi Caboni
Università degli studi di Cagliari
**115** PUBLICATIONS **1,555** CITATIONS
SEE PROFILE

Todd Sherer
Michael J. Fox Foundation for Parkinson's Re…
**53** PUBLICATIONS **5,926** CITATIONS
SEE PROFILE

Nanjing Zhang
PTC Therapeutics
**29** PUBLICATIONS **510** CITATIONS
SEE PROFILE

John Casida
University of California, Berkeley
**817** PUBLICATIONS **23,841** CITATIONS
SEE PROFILE

# Rotenone, Deguelin, Their Metabolites, and the Rat Model of Parkinson's Disease

Pierluigi Caboni,[†,‡] Todd B. Sherer,[§] Nanjing Zhang,[†] Georgia Taylor,[§] Hye Me Na,[§] J. Timothy Greenamyre,[§] and John E. Casida*[,†]

*Environmental Chemistry and Toxicology Laboratory, Department of Environmental Science, Policy and Management, University of California, Berkeley, California 94720-3112, and Emory Center for Neurodegenerative Disease, Emory University, Atlanta, Georgia 30322*

*Received May 14, 2004*

Rotenone and deguelin are the major active ingredients and principal components of cubé resin from *Lonchocarpus utilis* used as a botanical insecticide and piscicide. They are also potent complex I (NADH:ubiquinone oxidoreductase) inhibitors. Rotenone was known earlier, and deguelin is shown here to induce a Parkinson's disease (PD)-like syndrome after subcutaneous treatment of rats by osmotic minipump. Rotenone at 3 mg/kg/day or deguelin at 6 but not 3 mg/kg/day induces degeneration of the nigrostriatal dopaminergic pathway, as shown by reduced tyrosine hydroxylase immunoreactivity with treatments for 5 or 6 days. The neuropathological lesions are associated with a brain level of parent rotenoid of 0.4−1.3 ppm but not with the much smaller brain level of 12a$\beta$-hydroxyrotenoids or other metabolites analyzed by HPLC and LC/MS. We previously established that the hydroxylated metabolites and derivatives of rotenone and deguelin are all less active (i.e., detoxified) as complex I inhibitors relative to the parent rotenoids. The PD-like syndrome induced in rats by rotenone and deguelin is therefore due to the parent compounds rather than metabolites. Deguelin is about half as active as rotenone in inducing the PD-like syndrome in rats and in acute ip $LD_{50}$ in mice. Rotenone and deguelin are metabolized by human recombinant 3A4 and 2C19 but not five other P450 enzymes. 2C19 is more selective than 3A4 in forming the 12a$\beta$-hydroxyrotenoids. Identified sites of metabolic attack individually or in combination are as follows: 12a$\beta$ hydroxylation and 2-*O*-demethylation of both compounds, oxidation of the rotenone isopropenyl substituent to mono and diol derivatives, and probable oxidation of the deguelin dimethylchromene double bond. These toxicological features must be considered in using rotenone, deguelin, and their analogues as pesticides, candidate radioimaging and cancer chemopreventive agents, and models of PD.

## Introduction

Mitochondrial dysfunction, diminished complex I (NADH:ubiquinone oxidoreductase) activity, and oxidative stress in the brain are implicated as factors in the pathophysiology of Parkinson's disease (PD)[1] (*1*−*3*). The botanical insecticide and piscicide rotenone (*4*) (Figure 1), the classical mitochondrial complex I inhibitor, induces a PD-like syndrome on chronic subcutaneous treatment of rats (*5*). There is selective striatal oxidative damage and degeneration of the nigrostriatal dopaminergic pathway. The rotenone-exposed rats show symptoms of akinesia, rigidity, tremor, flexed posture, and piloerection. Their histopathology includes decreased striatal tyrosine hydroxylase (TH) immunoreactivity, degeneration of TH immunoreactive neurons in the substantia nigra pars compacta, some loss of locus ceruleus neurons, and formation of ubiquitin- and α-synuclein-positive inclusions in nigral cells, which are similar to the Lewy bodies of PD (*5*−*11*). In vitro models also show rotenone-induced mitochondrial impairment linked to altered $\beta$-synuclein metabolism and oxidative damage (*12*) and degeneration of dopaminergic neurons synergized by an inflammogen (*13*, *14*). These findings suggest that environmental toxins that inhibit complex I and cause chronic oxidative stress are candidate causes of PD.

Cubé resin, a root extract of *Lonchocarpus utilis* and *Lonchocarpus urucu*, is a principal commercial form of the botanical insecticide rotenone. Deguelin (Figure 1) is the second most important rotenoid in cubé resin in content and complex I inhibitory activity (*15*, *16*) and is also a prominent candidate antitumor and cancer chemopreventive agent as discussed later. The metabolism of rotenone in rat and fish liver microsomes involves cytochrome P450 (P450) oxidation at the 12a-, 8′-, and 6′,7′-positions (*17*, *18*), and there is also in vivo *O*-demethylation at the 2-position in mice (*19*, *20*) (Figure 1). No comparative information is available on the distribution and metabolic fate of rotenone vs deguelin or on the structure of the metabolites of deguelin.

* To whom correspondence should be addressed. Tel: 510-642-5424. Fax: 510-642-6497. E-mail: ectl@nature.berkeley.edu.
† University of California.
‡ Current address: Department of Toxicology, University of Cagliari, Sardinia, Italy.
§ Emory University.

[1] Abbreviations: 3A4 and related designations, P450 enzymes; P450, cytochrome P450; ESI, electrospray ionization; IgG, immunoglobulin; ODC, ornithine decarboxylase; PD, Parkinson's disease; PEG, poly(ethylene glycol); TH, tyrosine hydroxylase; $t_R$, retention time (min).

10.1021/tx049867r CCC: $27.50 
Published on Web 10/28/2004

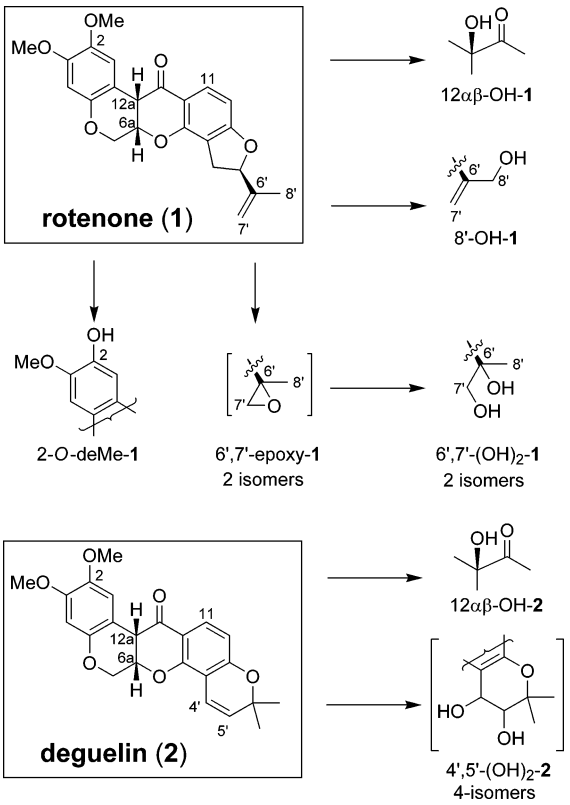


**Figure 1.** Structures of rotenone (**1**), deguelin (**2**), and some of their metabolites. The numbering system of **1** and its metabolites and derivatives is also used in the **2** series to simplify comparisons. Although not observed, 6′,7′-epoxy-**1** is an intermediate in the metabolism of **1**. The metabolites of **2** may include isomers of 4′,5′-$(OH)_2$-**2** and 12a$\beta$,4′,5′-$(OH)_3$-**2** in the region of Y-OH-**2**.

This study examines five aspects of rotenone, deguelin, and their metabolites in relation to the rat model of PD. First, is the rat model unique to rotenone or does deguelin also act the same way? Second, is there a sensitive and specific method for analysis of these rotenoids and their metabolites? Third, are the neurotoxicity and neuropathology related to the amount of parent rotenoid in the brain, considering both rats and mice? Next, do rotenoid metabolites in the brain contribute to the neurological effects? Finally, how are these rotenoids metabolized by human P450 enzymes as a bridge to interpreting the possible applicability of animal experiments to human PD?

## Materials and Methods

**Rotenoids. 1. Rotenone (1).** Rotenone (95−98% pure) was used as obtained from Sigma (St. Louis, MO) and had no toxicologically significant impurities.

**2. Preparation of Deguelin.** Deguelin (**2**) (97−99% pure and completely free of starting material) was prepared from rotenone by the three-step procedure of Anzeveno (*21*) (Scheme 1) with a simple modification of the first step (*22*) by addition of the boron tribromide solution into rotenone and maintainance for 10 min at −5 °C instead of rotenone into the boron tribromide solution and maintainance for 2 min at that temperature. This improvement provided consistency between different reactions and easy product isolation and purification in 20% overall yield.

**2.1. 8-(4-Bromo-3-methylbut-2-enyl)-9-hydroxy-2,3-dimethoxy-6a,12a-dihydro-6*H*-chromeno[3,4-*b*]chromen-12-one (3).** Into a solution of rotenone (4.00 g, 10.2 mmol) in dichloromethane (10 mL) below −5 °C was added a solution of boron tribromide in dichloromethane (1.0 M × 10.2 mL, 10.2 mmol).

**Scheme 1. Conversion of Rotenone (1) to Deguelin (2)**

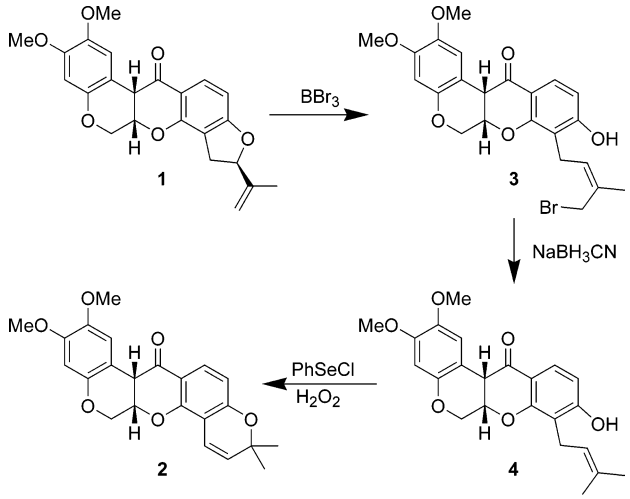


The mixture was stirred at −5 °C for 10 min, followed by removal of dichloromethane. The resulting brown to black residue was cooled with ice and treated with anhydrous methanol (20 mL). The mixture was filtered, and the solid (**3**) was collected and dried (3.10 g, 64%).

**2.2. 9-Hydroxy-8-(3-methylbut-2-enyl)-2,3-dimethoxy-6a,12a-dihydro-6*H*-chromeno[3,4-*b*]chromen-12-one (4).** Compound **3** from the above preparation (3.00 g, 6.3 mmol) was dissolved in hexamethylphosphoramide (32 mL), together with sodium cyanoborohydride (1.60 g, 25.4 mmol). The mixture was stirred at 80 °C for 2.5 h and then poured into ice−water. Extraction with ether/hexanes (3:1) followed by a wash with brine provided a solid, which was purified by column chromatography on silica gel with ethyl acetate and hexanes (1:1) to give **4** as a solid (1.50 g, 60%).

**2.3. Deguelin.** Compound **4** (1.50 g, 3.8 mmol) was dissolved in dichloromethane (45 mL) at −30 °C, and then, phenylselenenyl chloride (0.79 g, 4.1 mmol) was added. The solution was allowed to rise to room temperature over 2 h and stirred for an additional hour. The solvent was then removed, and THF (45 mL) was added, followed by 30% hydrogen peroxide (0.75 mL) at 0 °C. The mixture was stirred overnight at room temperature, followed by the addition of ethyl acetate (50 mL) and washing with 5% sodium bicarbonate and brine. The solvent was removed, and the residue was chromatographed with ethyl acetate and hexanes (1:2) to give deguelin (0.80 g, 53%).

**Systemic Administration of Rotenoids to Rats.** All animal use was in accordance with National Institutes of Health guidelines and was approved by the Emory University Institutional Animal Care and Use Committee. Male Lewis rats (275−350 g) (Charles River Laboratory, Wilmington, MA) were used for this study. Alzet osmotic minipumps (Alza, Palo Alto, CA) were filled with rotenone or deguelin dissolved in equal volumes of $Me_2SO$ and poly(ethylene glycol) (PEG-300; Sigma) or solvent alone. The pumps were incubated in sterile 0.9% saline at 37 °C overnight. Isoflurane (Abbott Laboratories, North Chicago, IL) was used as the anesthetic and euthanizing agent. One minipump was implanted under the skin on the back of each animal. The control rats received $Me_2SO$:PEG (1:1) only. The treated rats received 3.0 mg/kg/day rotenone or 3.0 or 6.0 mg/kg/day deguelin (calculated based on weight at the time of surgery). The delivery rate of $Me_2SO$:PEG was 2.5 and 5.0 $\mu$L/h for the 28 and up to 14 day experiments, respectively. In instances when rotenone- or deguelin-infused rats showed weight loss, the diet was supplemented with oral administration of Nutrical (Evsco Pharmaceuticals, Buena, NJ). Rats were usually euthanized after 14 or 28 days. In a few cases, they were sacrificed after 5 or 6 days when they developed akinesia or rigidity severe enough to preclude adequate feeding or grooming. Brains were dissected midsagitally. One hemisphere was fixed

in 4% paraformaldehyde and processed for immunocytochemistry, and the other was used along with a liver sample for analysis of rotenoid levels as described below. All samples for both types of analyses were coded in a blind study to rule out observer bias.

**Neuropathology.** Free-floating 40 $\mu$m sections were incubated in primary antibodies for 48 h, followed by a 1 h incubation with biotinylated secondary antibody. The avidin−biotin complex method was used to detect antigen signal (ABC Elite kit, Vector Laboratories, Burlingame, CA), and 3,3′-diaminobenzidine tetrachloride was used to visualize the final product. The primary antibody was mouse monoclonal against TH, the rate-limiting enzyme in dopamine biosynthesis (1:2000; Chemicon, Temecula, CA). The secondary antibody was biotinylated goat anti-mouse immunoglobulin (IgG). Sections from each animal were also processed for silver staining, a sensitive technique to look for degenerating neuronal processes and cell bodies, as described previously (*5*). Stained sections were examined using bright field microscopy, and captured images were examined with Zeiss Axiovision 3.0 software. The stained tissue sections from each animal were assessed for lesions by two independent raters who were blinded to the treatment group. For final output, the images were processed identically using Adobe Photoshop 5.5 software.

**Treatment of Mice.** Male Swiss−Webster mice (22−28 g) (Harlan Sprague−Dawley, San Diego, CA) were administered the test compounds ip using $Me_2SO$ as the carrier vehicle (20−40 $\mu$L), or $Me_2SO$ alone was injected (control). $LD_{50}$ values were determined at 24 h. Alternatively, brain and liver were dissected out and analyzed 2 h after treatment with rotenone or deguelin at 2 mg/kg, during which time there was generally complete recovery from poisoning.

**Extraction of Brain and Liver for Analysis of Rotenoids and Metabolites.** The brain hemisphere and liver were held frozen at −80 °C from the time of sacrifice until analysis. They were individually weighed, placed in a glass homogenizer, and homogenized in 100 mM phosphate buffer (pH 7.4) (3 mL for brain samples less than 0.5 g; 4 mL for brain and liver samples greater than 0.5 g). Each homogenized sample was then extracted with ethyl acetate (2 mL), and an aliquot (1 mL) of the emulsion was placed in a 1.5 mL Eppendorf tube and centrifuged (10000*g*, 5 min) for complete phase separation. The upper ethyl acetate layer was recovered and evaporated with nitrogen to near dryness. The extract and some precipitate were dissolved or resuspended in 50:50 acetonitrile/water (200 $\mu$L) and sonicated. The sample was then filtered [0.2 $\mu$m nylon membrane in 13 mm Acrodisc syringe filter (Paul Gelman, Ann Arbor, MI)] and subjected to HPLC analysis as below in comparison with standard curves for the parent rotenoid and its 12a$\beta$-hydroxy (12a$\beta$-OH) metabolite. Recovery efficiencies for rotenone, deguelin, and their 12a$\beta$-hydroxy metabolites from brain and liver were generally in the range of 85−95%. Two types of possible metabolites would not be analyzed by this procedure, i.e., those not recovered in ethyl acetate on extraction such as conjugates and ones with a retention time ($t_R$) greater than 20 min.

**Analyses.** For HPLC quantitative analysis of rotenoids, a Hewlett-Packard model 1050 liquid chromatograph was used fitted with a diode array detector model HP1040M and an Alltech (Deerfield, IL) ODS2 column (250 mm × 4.6 mm id, 5 $\mu$m particle size). Isocratic development was with water−acetonitrile (1:1) for 20 min to elute the rotenoids and an additional 20 min to complete the elution of an interfering peak. The sample injection volume was 100 $\mu$L with a flow rate of 1 mL/min. Quantitative analyses involved peak area comparisons with synthetic standards and absorbance measurements at 290 nm.

For LC/MS identification of rotenoids, a Finnigan-MAT model TSQ-700 triple quadrupole mass spectrometer was used with an electrospray ionization (ESI) source. The mobile phase of acetonitrile (50%) and aqueous 0.1% formic acid (50%) was pumped with a Perkin-Elmer (Norwalk, CT) model 250 HPLC to a Rheodyne (Cotati, CA) model 7125 injector with a 10 $\mu$L sample loop. Samples were analyzed on an Alltech ODS2 column (150 mm × 4.6 mm id, 3 $\mu$m particle size) at 0.2 mL/min with UV detection (HP 1050 series) at 290 nm prior to entering the source of the mass spectrometer operated at 5.0 kV potential. The heated capillary temperature was set at 350 °C, and nitrogen was used at a sheath gas pressure of 40 psi.

**Candidate Metabolites. 1. Rotenone Metabolites.** Ten candidate metabolites of rotenone were available as standards from our earlier studies and are designated by the position and substituent changes from the parent compound (**1**), i.e., 12a$\beta$-OH-**1**, 2-*O*-deMe-**1**, 8′-OH-**1**, 12a$\beta$,8′-(OH)$_2$-**1**, 6′,7′-(OH)$_2$-**1**, 12a$\beta$,6′,7′-(OH)$_3$-**1**, 11-OH-**1**, 12a$\alpha$-OH-**1**, 6′,7′-epoxy-**1**, and 6a,-12a-dehydro-**1** (*17*−*19*, *23*, *24*).

**2. Deguelin Metabolites.** 12a$\beta$-OH-**2** was isolated from cubé resin (*15*, *16*). Deguelin was oxidized with equimolar *m*-chloroperoxybenzoic acid in methylene dichloride followed by hydrolysis with potassium hydroxide or with excess dimethyldioxirane in acetone at −78 °C followed by hydrolysis with dilute hydrochloric acid at room temperature for HPLC comparison of the product mixtures with the P450 metabolites.

**Metabolism by Human Recombinant P450 Enzymes.** Human P450 Supersomes [baculovirus-infected insect cells (BTI-TN-5B1-4) containing human P450 cDNA] and insect cell control Supersomes were obtained from BD Biosciences (Woburn, MA). Recombinant P450 was coexpressed with P450 reductase and (except with 1A2 and 2D6) also with cytochrome b5. The enzymes were used as received with normalized P450 activities (pmol product for indicated substrate/min/pmol P450) stated as: 1A2 phenacetin *O*-deethylase 41.7; 2A6 coumarin 7-hydroxylase 19.3; 2B6 7-ethoxy-4-trifluoromethylcoumarin *O*-deethylase 9.7; 2C19 (*S*)-mephenytoin 4′-hydroxylase 11.8; 2C9 diclofenac 4′-hydroxylase 5.3; 2D6 (+/−)-bufuralol 1′-hydroxylase 36.2; 2E1 *p*-nitrophenol hydroxylase 12.2; and 3A4 testosterone 6$\beta$-hydroxylase 150. Each incubation mixture contained a single P450 (125 pmol of P450, 0.4−1.0 mg of protein) and NADPH (0 or 1.5 mM) in 100 mM phosphate buffer (pH 7.4) adding the substrate (2.5 $\mu$g) last as a solution in acetone (2.5 $\mu$L) (final assay volume 175 $\mu$L). There were two exceptions as recommended by BD Biosciences: the buffer was 100 mM Tris (pH 7.4) for the phosphate sensitive 2A6, and the substrate was used as a film on the reaction vessel for the acetone sensitive 2E1. Incubations were performed in plastic Eppendorf tubes (1.5 mL) for 60 min at 37 °C in air. The incubated mixtures were extracted with ethyl acetate (200 $\mu$L) and centrifuged, and an aliquot (60 $\mu$L) was subjected to HPLC and LC/MS as above. The sum of the peak areas at 290 nm was considered to be 100%, and the percent of this amount for individual peaks was determined. Data are shown as means ± SD for three or four replicates. As controls, rotenone and deguelin are stable on incubation with enzyme in the absence of NADPH for 60 min at 37 °C.

## Results

**PD-Like Syndrome from Rotenone and Deguelin in Rats.** Rotenone and deguelin were compared with subcutaneous treatments recording toxicity and neuropathology rating (Table 1). The integrity of the nigrostriatal dopaminergic system was analyzed using immunocytochemistry with antibodies against TH. Rotenone at 3 mg/kg/day, in a 28 day experiment involving 23 rats, resulted in five deaths, two lesions with punctate loss of TH staining, five smaller lesions or reduced TH staining, and 11 with no effect. The rotenone experiment was then repeated with eight rats and 14 days of treatment at 3 mg/kg/day, i.e., half the overall amount of rotenone, resulting in one death and two demonstrated nigrostriatal dopaminergic lesions. Deguelin at 3 and 6 mg/kg/day was compared with rotenone at 3 mg/kg/day using the 14 day protocol. Ten animals received 3 mg/kg/day

**Table 1. Brain and Liver Levels of Rotenone, Deguelin, and Their 12a$\beta$-Hydroxy Metabolites in Rats in Relation to Neuropathology Rating**

| rotenoid (ppm ± SD) [a] | | toxicity or neuropathology rating [b] | |
|---|---|---|---|
| brain | liver | individual | average |
| rotenone (3 mg/kg/day for 28 days) | | | |
| 0.42 ± 0.14 | 0.23 ± 0.07 | 0, 2, 2, 3, 3 | 2.00 |
| 0.24 ± 0.01 | 0.20 ± 0.05 | 0, 0, 1, 1, 3 | 1.00 |
| 0.21 ± 0.02 | 0.11 ± 0.07 | 0, 0, 0, 1, 3 | 0.80 |
| 0.14 ± 0.03 | 0.11 ± 0.02 | 0, 0, 0, 0, 1 | 0.20 |
| 0.08 ± 0.03 | 0.18 ± 0.10 | 0, 1, 3 | 1.33 |
| rotenone (3 mg/kg/day for up to 14 days) | | | |
| 0.13 ± 0.00 | 0.07 ± 0.04 | 0, 1, 1 | 0.67[c] |
| 0.08 ± 0.04 | 0.04 ± 0.00 | 0, 0, 0, 0 | 0 |
| deguelin (3 mg/kg/day for 14 days) | | | |
| 0.28 ± 0.03 | 0.10 ± 0.05 | 0, 0, 0, 0, 0 | 0 |
| 0.16 ± 0.05 | 0.05 ± 0.02 | 0, 0, 0, 0, 0 | 0 |
| deguelin (6 mg/kg/day for up to 14 days) | | | |
| 0.39 ± 0.08 | 0.13 ± 0.05 | 0, 1, 1, 1 | 0.75[c] |
| 0.24 ± 0.04 | 0.17 ± 0.14 | 0, 0, 0, 2 | 0.50[c] |

[a] Order based on decreasing amount of parent rotenoid in the brain. The 12a$\beta$-hydroxy metabolites always average 0.05 ppm or less for each experiment and tissue. [b] Ratings for 3−5 rats in each group: 0 refers to no effect, i.e., same as controls; 1 designates a small lesion or reduced TH staining; 2 refers to lesions with punctate loss of TH staining; and 3 designates death. [c] The symptomatic animals were sacrificed on day 5 or 6 of treatment for neuropathy rating.

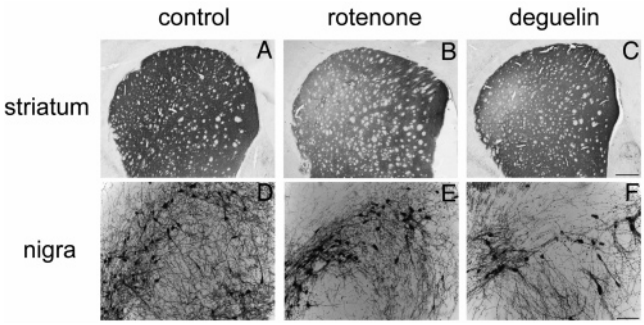


**Figure 2.** TH immunoreactivity in striatum and nigra of rotenoid-infused rats. The circumscribed loss of striatal TH is evident in the rotenoid-treated animals (B,C) vs the vehicle control (A). Fragmented varicose-like staining in the processes of nigral neurons is observed in rotenoid-treated animals (E,F) vs the control (D). The scale is shown by the bar in the far lower right corners of C (500 $\mu$m for A−C) and F (50 $\mu$m for D−F). Animals received vehicle (DMSO:PEG, 1:1), rotenone (3 mg/kg/day for 5 days), or deguelin (6 mg/kg/day for 6 days).

deguelin without evidence of nigrostriatal neurodegeneration. Of the nine animals that received 6 mg/kg/day deguelin, there was one death and four animals demonstrated evidence of nigrostriatal dopaminergic degeneration. Rotenone- and deguelin-treated animals with a dopaminergic lesion became hypokinetic and had unsteady movement, hunched posture, and in some cases severe rigidity (*5*). The overall incidence of PD-like syndrome was 39% of the 18 survivors with rotenone at 3 mg/kg/day for 28 days, 33% of the six survivors with rotenone at 3 mg/kg for up to 14 days, and 50% of the eight survivors with deguelin at 6 mg/kg/day for up to 14 days.

The neuropathological lesions are associated with reduced TH immunoreactivity in the nigrostriatal dopaminergic pathway as compared with vehicle-treated controls (Figure 2). This loss is evident in the striatrum with both rotenone at 3 mg/kg/day and deguelin at 6 mg/kg/day and includes symptomatic animals sacrificed at 5 or 6 days of treatment. In striatal regions where there was a loss of TH immunoreactivity, there was abnormal silver staining (not shown), indicative of degenerating nerve terminals, as stated before (*5*). Moreover, silver staining confirmed the preservation of postsynaptic striatal neurons (*5*, *11*). The selectivity and localization of the lesions were as previously described (*5*).

**Analysis of Rotenone and Deguelin and Their Metabolites.** The study of a possible relationship between the PD-like syndrome and the levels of rotenone, deguelin, and their metabolites in brain and liver required development of sensitive methods to quantitate and characterize the residues. Adequate separations for HPLC analyses were achieved on the ODS2 column eluted with acetonitrile:water (1:1) (Table 2 and Figure 3). The sensitivity limit (twice background) was 0.01 ppm for rotenone, deguelin, and their 12a$\beta$-OH derivatives based on peak areas at 290 nm, and there were no interfering materials.

HPLC and LC/MS were the critical methods for metabolite identification, matching $t_R$ values and ESI fragmentation patterns with authentic standards (Table 2 and Figure 3). Compounds with 12a-H give $[M + H]^+$ as a prominent peak or the base peak, and $[M + H + CH_3CN]^+$ is also observed. Those with 12a-OH give little or no $[M + H]^+$ and no $[M + H + CH_3CN]^+$; the major peak is $[M + H - H_2O]^+$. Identifications were verified by comparing the UV spectra of the metabolites with those of the standards.

**Brain and Liver Levels of Rotenone, Deguelin, and Their 12a$\beta$-Hydroxy Metabolites in Rats in Relation to Neuropathology Rating.** The investigations were designed to determine the possible relationship, if any, between the amount of parent rotenoid or metabolite in the brain and the neurotoxicity or neuropathology. The brain and liver levels of rotenone, deguelin, and their metabolites were determined by HPLC for rats with various toxicity or neuropathology ratings from the 14 or 28 day treatment regimens (Table 1). The brain levels of rotenone are generally higher after 28 than 14 days, averaging 0.22 and 0.11 ppm, respectively. The toxicity or neuropathology rating is also higher averaging 1.04 at 28 days and 0.29 at 14 days. The results for each experiment were then grouped from the highest to the lowest brain levels of rotenoid in sets of 3−5 animals. There is a general positive relationship between brain rotenoid level and severity of effect (Figure 4). The dose of 3 mg/kg/day for 28 days gave 0.1−0.4 ppm rotenone in the brain. The brain level was higher but not doubled for deguelin on going from 3 to 6 mg/kg/day for 14 days. The 12a$\beta$-OH metabolite levels in brain were much lower than the parent rotenoids, and no other metabolites were detected. Liver generally contained less parent rotenoid and metabolites than brain. The effect of deguelin at 6 mg/kg/day was nearly the same as that of rotenone at 3 mg/kg/day; thus, the subcutaneous toxicity in rats was about 2-fold greater for rotenone than deguelin.

**Brain and Liver Levels of Rotenone and Deguelin in Mice in Relation to Toxicity.** The ip $LD_{50}$ values in mice are 2.5 mg/kg for rotenone and 4.3 mg/kg for deguelin. The brain levels 2 h after ip administration at 2 mg/kg are 0.39 ± 0.27 and 0.18 ± 0.09 ppm ± SD for rotenone and deguelin, respectively. The liver levels are much lower at 0.05 ± 0.02 ppm ± SD. The 12a$\beta$-OH metabolites are the only ones detected and are minor

**Table 2. HPLC and LC/MS Characteristics of Rotenone (1), Deguelin (2), and Some of Their Candidate Metabolites**

| compound[a] | HPLC $t_R$ (min) | mol wt | LC/MS (ESI) *m/z* (% relative abundance) |
|---|---|---|---|
| rotenone | 15.67 | 394 | 395 $[M + H]^+$ 100, 436 $[M + H + CH_3CN]^+$ 5 |
| | | P450 metabolites of rotenone | |
| 12a$\beta$-OH-**1** | 10.14 | 410 | 393 $[M + H - H_2O]^+$ 100 |
| 2-*O*-deMe-**1** | 9.69 | 380 | 381 $[M + H]^+$ 100, 422 $[M + H + CH_3CN]^+$ 18 |
| X-OH-**1** | 9.01 | | 270 (100), 311 (95), 411 (90), 301 (16), 344 (14), 379 (7) |
| Y-OH-**1** | 6.92 | | 311 (100), 379 (98), 270 (82), 301 (32), 344 (26), 452 (5) |
| 8′-OH-**1** | 5.13 | 410 | 411 $[M + H]^+$ 100, 452 $[M + H + CH_3CN]^+$ 8 |
| 12a$\beta$,8′-$(OH)_2$-**1** | 3.95 | 426 | 409 $[M + H - H_2O]^+$ 100, 427 $[M + H]^+$ 5 |
| 6′,7′-$(OH)_2$-**1** | 3.54, 3.38 [c] | 428 | 429 $[M + H]^+$ 100, 470 $[M + H + CH_3CN]^+$ 6 |
| 12a$\beta$,6′,7′-$(OH)_3$-**1** | 2.98, 2.81 [c] | 444 | 427 $[M + H - H_2O]^+$ 100 |
| | | not identified as metabolites of rotenone | |
| 11-OH-**1** | 16.10 | 410 | 411 $[M + H]^+$ 100, 452 $[M + H + CH_3CN]^+$ 82 |
| 12aα-OH-1 | 14.94 | 410 | 393 $[M + H - H_2O]^+$ 100 |
| 6′,7′-epoxy-**1** | 7.59, 7.88 [d] | 410 | 411 $[M + H]^+$ 100, 452 $[M + H + CH_3CN]^+$ 14 |
| 6a,12a-dehydro-**1** | 34.04 | 392 | 393 $[M + H]^+$ 100 |
| deguelin | 18.24 | 394 | 395 $[M + H]^+$ 100, 436 $[M + H + CH_3CN]^+$ 10 |
| | | P450 metabolites of deguelin | |
| 12a$\beta$-OH-**2** | 11.38 | 410 | 393 $[M + H - H_2O]^+$ 100 |
| 2-*O*-deMe-**2** | 10.37 | 380 | 381 $[M + H]^+$ 100, 422 $[M + H + CH_3CN]^+$ 7 |
| X-OH-**2** | 7.40 | | 379 (100), 393 (13) |
| Y-OH-**2** | 3.38 | | mixture[e] |
| | | not identified as metabolites of deguelin | |
| 11-OH-**2** | 26.38 | 410 | 411 $[M + H]^+$ 100, 452 $[M + H + CH_3CN]^+$ 43 |
| 12aα-OH-**2** | 17.40 | 410 | 393 $[M + H - H_2O]^+$ 100 |
| 6a,12a-dehydro-**2** | 41.88 | 392 | 393 $[M + H]^+$ 100 |

[a] Metabolites indicated by structure are assigned by $t_R$, MS fragmentation, and UV spectral comparisons with synthetic standards. As the only exception, 2-*O*-deMe-**2** is assigned by MS fragmentation of the metabolite and analogy with the findings for 2-*O*-deMe-**1**. Common names or other literature designations are as follows: 12a$\beta$- and 12aα-OH-**1**, rotenolones I and II; 12a$\beta$- and 12aα-OH-**2**, tephrosins I and II; 11-OH-**1** and 11-OH-**2**, sumatrol and α-toxicarol. [b] Identified in this study as P450 metabolites of rotenone and deguelin in human liver 3A4- and 2C19-NADPH systems. [c] Partially resolved metabolites suggested to be isomers with the same fragmentation pattern. [d] Resolved isomers with the same fragmentation pattern. [e] Mixture apparently containing one or more isomers of both 4′,5′-$(OH)_2$-**2** (from dimethyldioxirane oxidation and acid hydrolysis) MS *m/z* 429 $[M + H]^+$ 100, 470 $[M + H + CH_3CN]^+$ 32 and 12a$\beta$,4′,5′-$(OH)_3$-**2** (from 3A4) MS *m/z* 427 $[M + H - H_2O]^+$ 100, 409 (26), 392 (20).

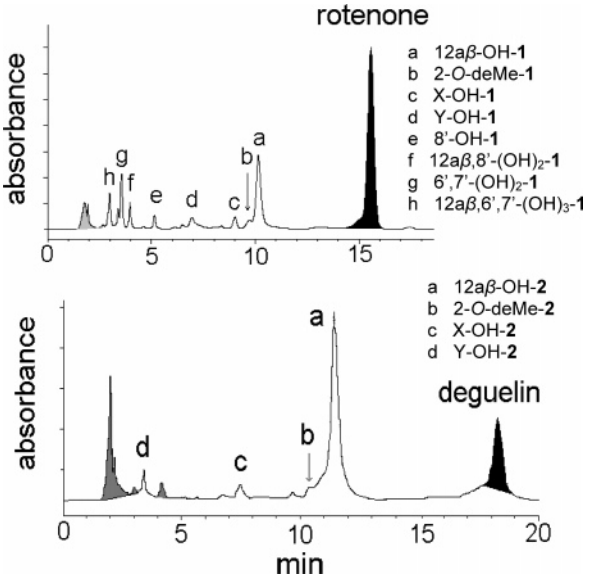


**Figure 3.** Representative HPLC chromatograms of rotenone and deguelin metabolites in human recombinant 3A4-NADPH systems. No metabolites are observed without NADPH fortification. The shaded peaks contain interfering materials and are therefore not included in quantification of the metabolites.

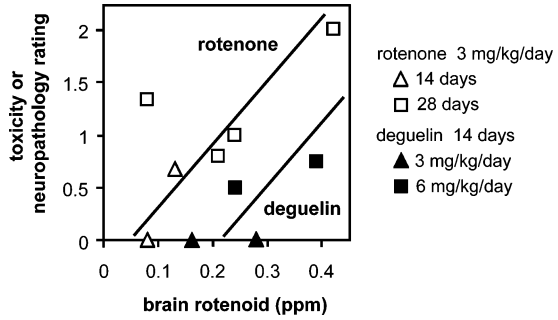


**Figure 4.** Relation between brain level of rotenone or deguelin and neuropathology rating in rats. Data from Table 1 are plotted with brain ppm levels of parent rotenoid vs average toxicity or neuropathology ratings.

(<0.01 ppm for each compound and tissue, $n = 9$ or 10) relative to the parent rotenoids.

**Metabolism of Rotenone and Deguelin by Human Recombinant P450 Enzymes.** Incubation of rotenone or deguelin with 3A4 in the presence but not in the absence of NADPH yields several metabolites based on HPLC analysis (Figure 3). For rotenone metabolism, 3A4 is more active than the other P450 enzymes, which decrease in activity in the order: 3A4 > 2C19 > 2B6 or 2D6 > 1A2 > 2A6 or 2E1 (inactive) (Table 3). For deguelin metabolism, 2C19 is distinctly more effective than 3A4 and the other five enzymes are much less active or inactive (Table 4). The site selectivity varies for the P450 enzymes with 2C19 more specific than 3A4 for 12a$\beta$ hydroxylation of both rotenoids.

Several metabolites of rotenone are structurally assigned (Figure 1) by comparison with authentic standards on HPLC cochromatography (Figure 3) and as LC (ESI) fragmentation patterns (Table 2) and UV spectra (data not shown). The elution pattern is first the trihydroxy compounds and then dihydroxy and monohydroxy derivatives followed by the parent rotenoid (Figure 3). Major metabolites of rotenone are the 12a$\beta$-OH derivative per se and with additional sites of oxidation (Tables 2 and 3). 2-*O*-deMe-**1** is a minor metabolite. The isopro-

**Table 3. Metabolism of Rotenone by Human Recombinant P450 Enzymes**

| rotenoid | rotenoid composition (%)[a] with indicated P450 enzyme[b] | | | | |
|---|---|---|---|---|---|
| | 1A2 | 2B6 | 2C19 | 2D6 | 3A4 |
| rotenone | 94.2 ± 6.8 | 87.2 ± 23.8 | 70.4 ± 8.0 | 90.2 ± 11.9 | 61.9 ± 12.2 |
| 12a$\beta$-OH-**1** | 4.4 ± 0.1 | 6.0 ± 1.0 | 21.5 ± 1.0 | 4.8 ± 0.9 | 16.7 ± 2.8 |
| Y−OH-**1** | <0.05 | <0.05 | 2.8 ± 0.6 | <0.05 | 2.4 ± 0.8 |
| 8′-OH-**1** | 0.4 ± 0.1 | 0.6 ± 0.1 | 0.9 ± 0.2 | 1.9 ± 0.1 | 1.7 ± 0.3 |
| 6′,7′-$(OH)_2$-**1** | 0.3 ± 0.1 | 4.3 ± 0.4 | 1.7 ± 0.5 | <0.05 | 4.9 ± 0.7 |
| 6′,7′-$(OH)_2$-**1** | 0.7 ± 0.1 | 1.9 ± 0.2 | 1.3 ± 0.3 | 3.1 ± 0.2 | 1.8 ± 0.2 |
| 12a$\beta$,6′,7′-$(OH)_3$-**1** | <0.05 | <0.05 | 1.4 ± 0.4 | <0.05 | 3.5 ± 0.8 |
| other | <0.05 | <0.05 | <0.05 | <0.05 | 7.1 ± 1.1[c] |

[a] Mean ± SD ($n$ = 3) for NADPH-dependent metabolism. [b] 2A6 and 2E1 inactive. [c] Additional identified metabolites with 3A4 (% ± SD) are 2-*O*-deMe-**1** (1.6 ± 0.2) and 12a$\beta$,8′-$(OH)_2$-**1** (2.4 ± 0.4). Other metabolites detected with 3A4 but not the other P450 enzymes and therefore not given in the table are ($t_R$ min, % ± SD): X-OH-**1** (9.01, 1.8 ± 0.3), unknown (8.36, 0.4 ± 0.1), unknown (6.49, 0.5 ± 0.1), and unknown (4.59, 0.4 ± 0.1).

**Table 4. Metabolism of Deguelin by Human Recombinant P450 Enzymes**

| rotenoid | rotenoid composition (%)[a] with indicated P450 enzyme[b] | |
|---|---|---|
| | 2C19 | 3A4 |
| deguelin | <0.05 | 33.8 ± 11.5 |
| 12a$\beta$-OH-**2** | 56.9 ± 16.1 | 56.7 ± 37.4 |
| 2-*O*-deMe-**2** | <0.05 | 2.4 ± 0.1 |
| X-OH-**2** | 43.1 ± 7.5 | 2.8 ± 0.1 |
| Y−OH-**2** | <0.05 | 4.3 ± 0.9 |

[a] Mean ± SD ($n$ = 4) for NADPH-dependent metabolism. [b] 1A2, 2A6, 2B6, 2D6, and 2E1 are less active or inactive.

penyl substituent of rotenone is oxidized at the double bond or methyl group in the formation of 8′-OH-**1**, 12a$\beta$,8′-$(OH)_2$-**1**, 6′,7′-$(OH)_2$-**1** (two isomers), and 12a$\beta$,6′,7′-$(OH)_3$-**1** (two isomers). X-OH-**1** appears to be a monohydroxy derivative ($[M + H]^+$ *m/z* 411 and appropriate $t_R$ value) such as at the benzylic methylene C-4′. Y-OH-**1** is related to X-OH-**1** by somewhat similar fragmentation and may be a dihydroxy compound such as 12a$\beta$,4′-$(OH)_2$-**1**.

12a$\beta$-OH-**2** is the major metabolite of deguelin with 3A4 (Figure 3) and the more active 2C19 (Tables 2 and 4). The metabolites of deguelin are similar chromatographically to the mono-, di-, and triol derivatives of rotenone (Figure 3). 2C19 gives a large amount of X-OH-**2** relative to 3A4 (Table 4). The structures are not assigned for X-OH-**2** and Y-OH-**2**. They may each be poorly resolved isomeric mixtures but appear to be generally analogous to Y-OH-**1** and 12a$\beta$,6′,7′-$(OH)_3$-**1**, respectively. One component of the 3A4-deguelin metabolite mixture may be an isomer of 12a$\beta$,4′,5′-$(OH)_3$-**2** (Table 2). Dimethyldioxirane followed by acid hydrolysis was more effective than *m*-chloroperoxybenzoic acid and alkaline hydrolysis in the conversion of deguelin to a mixture of products in the chromatographic region of Y-OH-**2**, one of which is probably an isomer of 4′,5′-$(OH)_2$-**2** (Table 2).

## Discussion

**Rotenone and Deguelin Are the Two Most Important Rotenoids.** These rotenoids differ only in the dihydrofuran vs pyran ring with substituents (Figure 1), and the chemical conversion of rotenone to deguelin is a principal means of obtaining high purity deguelin (*21*). The rotenone:deguelin ratio in cubé resin is 2.0 (*15*), but it varies greatly from other plant sources and parts (*25*, *26*).

Rotenone and deguelin have several types of activities in addition to pest control. On chronic feeding, rotenone reduces the incidence of spontaneous mammary tumors in rats and inhibits cell proliferation in mouse liver (*27*−*29*), suggesting cancer chemopreventive action. Deguelin is a potent inhibitor of phorbol ester-induced ornithine decarboxylase (ODC) activity (*30*) and is effective in several in vitro and in vivo experimental models of carcinogenesis (*30*−*39*). The potency of deguelin is similar to that of rotenone for inhibiting complex I activity and ODC induction (*16*, *40*). More generally, all of the rotenoids in cubé resin have nearly the same structural specificity for inhibiting complex I activity and ODC induction (*15*, *16*). A family of potent 2,2-dimethylbenzopyran-based (i.e., deguelin analog) complex I inhibitors was prepared as potential cancer chemopreventive agents (*41*). Rotenone has been a prototype for preparing [$^3$H]-, [$^{11}$C]-, [$^{18}$F]-, and [$^{125}$I]-candidates for radioimaging of the brain and heart (*42*−*48*). Knowledge of the metabolism of rotenone and deguelin will help optimize these probes.

**Rotenoid Model of PD.** The rotenone model of PD is based on chronic treatment in rats, leading to selective degeneration of the nigrostriatal dopaminergic pathway and formation of ubiquitin- and α-synuclein-positive inclusions in nigral cells, which are similar to Lewy bodies (*5*). TH immunocytochemistry and silver staining show that deguelin causes similar PD-like nigrostriatal degeneration to that from rotenone, although at a somewhat higher dose (this study), and is therefore added to the list of chemicals that can model aspects of PD in rats. Although we did not measure levels of dopamine and its metabolites, the combination of TH and silver staining provides compelling evidence for the loss of nigrostriatal terminals in the deguelin-treated rats. This is the first demonstration of deguelin-induced toxicity to the nigrostriatal dopaminergic system. It is also noteworthy that silver staining failed to reveal any pathology outside the nigrostriatal system (not shown). The high selectivity for the nigrostriatal dopaminergic system vs postsynaptic striatal neurons, which is characteristic of idiopathic PD, is reportedly not seen with rotenone and other compounds giving generalized complex I inhibition in studies with rats using a somewhat different experimental protocol than in the present investigation (*49*−*51*). Mice administered rotenone acutely do not show a PD-like syndrome (*52*) although ip-administered rotenone readily passes the blood−brain barrier (this study). Although not specifically examined, this may be due to faster metabolism of rotenone in mice vs rats.

**Brain and Liver Levels of Rotenoids and Metabolites in Relation to Toxicity and Neuropathology Rating.** The neuropathology ratings and systemic toxicity in rats are generally greater with increasing levels of rotenone and deguelin in the brain (Figure 4). A level of

0.4 ppm is associated with a greatly increased incidence of degeneration of the nigrostriatal dopaminergic pathway and punctate TH lesions in the striatum, with rotenone somewhat more potent than deguelin. The 12a$\beta$-OH rotenoids are the only metabolites detected in the brain. There is little or no relation between rotenoid level in the liver and neuropathology rating. We previously established that the hydroxylated metabolites and derivatives of rotenone and deguelin are all less active (i.e., detoxified) as complex I inhibitors relative to the parent rotenoids (*15*−*18*, *23*, *24*). These overall findings therefore show that the PD-like syndrome induced in rats by rotenone and deguelin is associated with the brain levels of the parent compounds rather than that of any specific metabolites.

[$^3$H]Dihydrorotenone labels complex I in rat brain slices (*42*, *43*) and in vivo (*44*) with much less binding in rotenone-poisoned animals. [$^3$H]Deguelin has a relatively long residence time in the heart and fat relative to the total radioactivity with excretion mostly as unidentified metabolites (*33*). On comparing rotenone and deguelin in mice as single ip doses of 2 mg/kg in the present study, the level of rotenone in the brain is about twice that of deguelin, consistent with the 2-fold higher toxicity of rotenone than deguelin. An $LD_{50}$ dose of rotenone (2.5 mg/kg) administered ip in mice shows within 20 min a nearly complete block of mitochondrial respiration (pyruvate oxidation) in the brain (*53*).

**Metabolism of Rotenone and Deguelin by Human Recombinant P450 Enzymes.** The studies included most of the major human liver P450 enzymes showing the highest activity on rotenone and deguelin for 3A4 and 2C19, with the other five enzymes examined being much less active. A major metabolic reaction for both rotenone and deguelin is hydroxylation at the 12a-position to form 12a$\beta$-OH-**1** and 12a$\beta$-OH-**2**. 12a$\alpha$-OH-**1** is not observed or is very minor in the present study. Earlier reports of 12a$\alpha$-OH-**1** as a metabolite of rotenone (*17*, *18*) may be due in part to atmospheric or photochemical oxidation on TLC analysis. *O*-Demethylation is observed in the 2-position of rotenone with 3A4 (this study) and in vivo (*19*).

Deguelin metabolism involves conversion to 12a$\beta$-OH-**2** and probably also *O*-demethyl-**2** although a standard *O*-demethyl derivative was not available. An additional site of metabolic attack is likely to be the 4′,5′-double bond undergoing epoxidation and cleavage to the diol isomers [4′,5′-$(OH)_2$-**2** derivatives] (Figure 1). The dimethylchromene system of deguelin is shared by the precocenes (7-methoxy-2,2-dimethyl-3-chromene and the 6,7-dimethoxy analogue), which are metabolized in insects to give, as major products, the cis and trans 3,4-dihydro-3,4-dihydroxy and 3,4-dihydro-4-hydroxy derivatives (*54*, *55*). All four isomers of 12a$\beta$,4′,5′-$(OH)_3$-**2** are present along with deguelin and 12a$\beta$-OH-**2** in cubé resin (*16*). It therefore appears likely that the P450 metabolites of deguelin include one or more isomers of each of 4′,5′-$(OH)_2$-**2** and 12a$\beta$,4′,5′-$(OH)_3$-**2**.

**Importance of P450 in Limiting Rotenoid Potency.** Three observations indicate that P450 detoxification is a major factor in limiting rotenone toxicity. First, the P450 inhibitor piperonyl butoxide blocks metabolism in a microsome-NADPH system (*18*) and greatly increases the toxicity of rotenone in mice (*56*). Second, piperonyl butoxide is sometimes added to rotenone for enhanced effectiveness as an insecticide and piscicide. Third, as noted above, the metabolites of rotenone are all less active, so prolonging high levels of the parent compound increases toxicity. Therefore, because metabolites are a small contribution to overall rotenoid levels in the brain and considering their activity relative to the parent compounds, they are probably not contributors to complex I inhibition or coupled events. Interestingly, P450 polymorphisms have been implicated in PD pathogenesis, although this remains controversial (*57*).

## Conclusions

The two major rotenoids in the commercial cubé resin pesticide are rotenone and deguelin. They are of similar potency as acute toxicants and inhibitors of complex I and induced ODC activity and in producing degeneration of the nigrostriatal dopaminergic pathway in the PD rat model. Each type of activity is due to the parent rotenoid rather than a metabolite. Rotenone and deguelin are readily oxidized by human 3A4 and 2C19 with different site specificities for the two substrates. Detoxification is an important factor in reducing potency and toxicity. These toxicological features must be considered in using rotenone, deguelin, and their analogues as pesticides, candidate radioimaging and cancer chemopreventive agents, and models of PD.

**Acknowledgment.** The studies at Berkeley were supported by Grant 1 U54 ES12078 from the National Institute of Environmental Health Sciences (NIEHS), NIH, in collaboration with Marie-Francoise Chesselet and Jeff Bronstein of the Department of Neurology, School of Medicine, University of California at Los Angeles. The work at Emory was supported by 1 U54 ES012068 and a Michael J. Fox Foundation Fellowship. The contents of this paper are solely the responsibility of the authors and do not necessarily represent the official views of the NIEHS. We acknowledge the advice and assistance of Ryan Dick, Richard Staub, Rebecka Klintenberg, Nianbai Fang, and Gary Quistad, current or former members of the Berkeley laboratory. We also thank Professor Paolo Cabras of the University of Cagliari, Italy, for continuing interest in this research.

## References

(1) Schapira, A. H. V., Cooper, J. M., Dexter, D., Clark, J. B., Jenner, P., and Marsden, C. D. (1990) Mitochondrial complex I deficiency in Parkinson's disease. *J. Neurochem. 54*, 823−827.

(2) Beal, M. F., Howell, N., and Bódis-Wollner, I., Eds. (1997) *Mitochondria and Free Radicals in Neurodegenerative Diseases*, Wiley-Liss, New York.

(3) Olanow, C. W., and Tatton, W. G. (1999) Etiology and pathogenesis of Parkinson's disease. *Annu. Rev. Neurosci. 22*, 123−144.

(4) Tomlin, C. D. S., Ed. (2003) *The Pesticide Manual*, 13th ed., British Crop Protection Council, Alton, Hampshire, United Kingdom.

(5) Betarbet, R., Sherer, T. B., MacKenzie, G., Garcia-Osuna, M., Panov, A. V., and Greenamyre, J. T. (2000) Chronic systemic pesticide exposure reproduces features of Parkinson's disease. *Nat. Neurosci. 3*, 1301−1306.

(6) Betarbet, R., Sherer, T. B., and Greenamyre, J. T. (2002) Animal models of Parkinson's disease. *BioEssays 24*, 308−318.

(7) Sherer, T. B., Betarbet, R., and Greenamyre, J. T. (2002) Environment, mitochondria, and Parkinson's disease. *Neuroscientist 8*, 192−197.

(8) Alam, M., and Schmidt, W. J. (2002) Rotenone destroys dopaminergic neurons and induces parkinsonian symptoms in rats. *Behav. Brain Res. 136*, 317−324.

(9) Greenamyre, J. T., Betarbet, R., and Sherer, T. B. (2003) The rotenone model of Parkinson's disease: Genes, environment and mitochondria. *Parkinsonism Relat. Disord. 9*, S59−S64.

(10) Sherer, T. B., Betarbet, R., Kim, J.-H., and Greenamyre, J. T. (2003) Selective microglial activation in the rat rotenone model of Parkinson's disease. *Neurosci. Lett. 341*, 87−90.
(11) Sherer, T. B., Kim, J.-H., Bertarbet, R., and Greenamyre, J. T. (2003) Subcutaneous rotenone exposure causes highly selective dopaminergic degeneration and α-synuclein aggregation. *Exp. Neurol. 179*, 9−16.
(12) Sherer, T. B., Betarbet, R., Stout, A. K., Lund, S., Baptista, M., Panov, A. V., Cookson, M. R., and Greenamyre, J. T. (2002) An in vitro model of Parkinson's disease: Linking mitochondrial impairment to altered α-synuclein metabolism and oxidative damage. *J. Neurosci. 22*, 7006−7015.
(13) Gao, H.-M., Hong, J.-S., Zhang, W., and Liu, B. (2003) Synergistic dopaminergic neurotoxicity of the pesticide rotenone and inflammogen lipopolysaccharide: relevance to the etiology of Parkinson's disease. *J. Neurosci. 23*, 1228−1236.
(14) Gao, H.-M., Liu, B., and Hong, J.-S. (2003) Critical role for microglial NADPH oxidase in rotenone-induced degeneration of dopaminergic neurons. *J. Neurosci. 23*, 6181−6187.
(15) Fang, N., and Casida, J. E. (1998) Anticancer action of cubé insecticide: Correlation for rotenoid constituents between inhibition of NADH:ubiquinone oxidoreductase and induced ornithine decarboxylase activities. *Proc. Natl. Acad. Sci. U.S.A. 95*, 3380−3384.
(16) Fang, N., and Casida, J. E. (1999) Cubé resin insecticide: Identification and biological activity of 29 rotenoid constituents. *J. Agric. Food Chem. 47*, 2130−2136.
(17) Fukami, J.-I., Yamamoto, I., and Casida, J. E. (1967) Metabolism of rotenone *in vitro* by tissue homogenates from mammals and insects. *Science 155*, 713−716.
(18) Fukami, J.-I., Shishido, T., Fukunaga, K., and Casida, J. E. (1969) Oxidative metabolism of rotenone in mammals, fish, and insects and its relation to selective toxicity. *J. Agric. Food Chem. 17*, 1217−1226.
(19) Unai, T., Cheng, H.-M., Yamamoto, I., and Casida, J. E. (1973) Chemical and biological *O*-demethylation of rotenone derivatives. *Agric. Biol. Chem. 37*, 1937−1944.
(20) Carson, D., Crombie, L., and Whiting, D. A. (1975) Reaction of rotenone with boron tribromide. Stereospecific $^2$H-labeling of (−)-rotenonic acid in the 4′(*E*)-methyl group. *J. Chem. Soc., Chem. Commun.*, 851−852.
(21) Anzeveno, P. B. (1979) Rotenoid interconversion. Synthesis of deguelin from rotenone. *J. Org. Chem. 44*, 2578−2580.
(22) Unai, T., and Yamamoto, I. (1973) Synthesis of the stereoisomers of natural rotenone. *Agric. Biol. Chem. 37*, 897−901.
(23) Yamamoto, I., Unai, T., Ohkawa, H., and Casida, J. E. (1971) Stereochemical considerations in the formation and biological activity of the rotenone metabolites. *Pestic. Biochem. Physiol. 1*, 143−150.
(24) Unai, T., Yamamoto, I., Cheng, H.-M., and Casida, J. E. (1973) Synthesis and stereochemical characterization of hydroxy- and epoxy-derivatives of rotenone. *Agric. Biol. Chem. 37*, 387−401.
(25) Metcalf, R. L. (1955) *Organic Insecticides: Their Chemistry and Mode of Action*, Interscience, New York.
(26) Delfel, N. E., Tallent, W. H., Carlson, D. G., and Wolff, I. A. (1970) Distribution of rotenone and deguelin in *Tephrosia vogelii* and separation of rotenoid-rich fractions. *J. Agric. Food Chem. 18*, 385−390.
(27) Hansen, W. H., Davis, K. J., and Fitzburgh, O. G. (1965) Chronic toxicity of cubé. *Toxicol. Appl. Pharmacol. 7*, 535−542.
(28) Cunningham, M. L., Soliman, M. S., Badr, M. Z., and Matthews, H. B. (1995) Rotenone, an anticarcinogen, inhibits cellular proliferation but not peroxisome proliferation in mouse liver. *Cancer Lett. 95*, 93−97.
(29) Schuler, F., and Casida, J. E. (2001) The insecticide target in the PSST subunit of complex I. *Pest Manage. Sci. 57*, 932−940.
(30) Luyengi, L., Lee, I.-S., Mar, W., Fong, H. H. S., Pezzuto, J. M., and Kinghorn, A. D. (1994) Rotenoids and chalcones from *Mundulea sericea* that inhibit phorbol ester-induced ornithine decarboxylase activity. *Phytochemistry 36*, 1523−1526.
(31) Gerhäuser, C., Mar, W., Lee, S. K., Suh, N., Luo, Y., Kosmeder, J., Luyengi, L., Fong, H. H. S., Kinghorn, A. D., Moriarty, R. M., Mehta, R. G., Constantinou, A., Moon, R. C., and Pezzuto, J. M. (1995) Rotenoids mediate potent cancer chemopreventive activity through transcriptional regulation of ornithine decarboxylase. *Nat. Med. 1*, 260−266.
(32) Udeani, G. O., Gerhäuser, C., Thomas, C. F., Moon, R. C., Kosmeder, J. W., Kinghorn, A. D., Moriarty, R. M., and Pezzuto, J. M. (1997) Cancer chemopreventive activity mediated by deguelin, a naturally occurring rotenoid. *Cancer Res. 57*, 3424−3428.
(33) Udeani, G. O., Zhao, G.-M., Shin, Y. G., Kosmeder, J. W., II, Beecher, C. W. W., Kinghorn, A. D., Moriarty, R. M., Moon, R. C., and Pezzuto, J. M. (2001) Pharmacokinetics of deguelin, a cancer chemopreventive agent in rats. *Cancer Chemother. Pharmacol. 47*, 263−268.
(34) Murillo, G., Salti, G. I., Kosmeder, J. W., II, Pezzuto, J. M., and Mehta, R. G. (2002) Deguelin inhibits the growth of colon cancer cells through the induction of apoptosis and cell cycle arrest. *Eur. J. Cancer 38*, 2446−2454.
(35) Mehta, R. G., and Pezzuto, J. M. (2002) Discovery of cancer chemopreventative agents from natural products: From plants to prevention. *Curr. Oncol. Rep. 4*, 478−486.
(36) Murillo, G., Kosmeder, J. W., II, Pezzuto, J. M., and Mehta, R. G. (2003) Deguelin suppresses the formation of carcinogen-induced aberrant crypt foci in the colon of CF-1 mice. *Int. J. Cancer 104*, 7−11.
(37) Chun, K.-H., Kosmeder, J. W., II, Sun, S., Pezzuto, J. M., Lotan, R., Hong, W. K., and Lee, H.-Y. (2003) Effects of deguelin on the phosphatidylinositol 3-kinase/Akt pathway and apoptosis in premalignant human bronchial epithelial cells. *J. Natl. Cancer Inst. 95*, 291−302.
(38) Lee, H.-Y., Suh, Y.-A., Kosmeder, J. W., Pezzuto, J. M., Hong, W. K., and Kurie, J. M. (2004) Deguelin-induced inhibition of cyclooxygenase-2 expression in human bronchial epithelial cells. *Clin. Cancer Res. 10*, 1074−1079.
(39) Ito, C., Itoigawa, M., Kojima, N., Tan, H. T.-W., Takayasu, J., Tokuda, H., Nishino, H., and Furukawa, H. (2004) Cancer chemopreventive activity of rotenoids form *Derris trifoliata*. *Planta Med. 70*, 8−11.
(40) Rowlands, J. C., and Casida, J. E. (1998) NADH:ubiquinone oxidoreductase inhibitors block induction of ornithine decarboxylase activity in MCF-7 human breast cancer cells. *Pharmacol. Toxicol. 83*, 214−219.
(41) Nicolaou, K. C., Pfefferkorn, J. A., Schuler, F., Roecker, A. J., Cao, G.-Q., and Casida, J. E. (2000) Combinatorial synthesis of novel and potent inhibitors of NADH:ubiquinone oxidoreductase. *Chem. Biol. 7*, 979−992.
(42) Greenamyre, J. T., Higgins, D. S., and Eller, R. V. (1992) Quantitative autoradiography of dihydrorotenone binding to complex I of the electron transport chain. *J. Neurochem. 59*, 746−749.
(43) Higgins, D. S., Jr., and Greenamyre, J. T. (1996) [$^3$H]Dihydrorotenone binding to NADH: ubiquinone oxidoreductase (complex I) of the electron transport chain: An autoradiographic study. *J. Neurosci. 16*, 3807−3816.
(44) Talpade, D. J., Greene, J. G., Higgins, D. S., Jr., and Greenamyre, J. T. (2000) In vivo labeling of mitochondrial complex I (NADH: ubiquinone oxidoreductase) in rat brain using [$^3$H]dihydrorotenone. *J. Neurochem. 75*, 2611−2621.
(45) Charalambous, A., Mangner, T. J., and Kilbourn, M. R. (1995) Synthesis of (2-[$^{11}$C]methoxy)-rotenone, a marker of mitochondrial complex I activity. *J. Nucl. Med. Biol. 22*, 65−69.
(46) Charalambous, A., Tluczek, L., Frey, K. A., Higgins, D. S., Jr., Greenamyre, T. J., and Kilbourn, M. R. (1995) Synthesis and biological evaluation in mice of (2-[$^{11}$C]methoxy)-6′,7′-dihydrorotenol, a second generation rotenoid for marking mitochondrial complex I activity. *J. Nucl. Med. Biol. 22*, 491−496.
(47) Martarello, L., Greenamyre, J. T., and Goodman, M. M. (1999) Synthesis and evaluation of a new fluorine-18 labeled rotenoid as a potential PET probe of mitochondrial complex I activity. *J. Labelled Compd. Radiopharm. 42*, 1039−1051.
(48) Marshall, R. C., Powers-Risius, P., Reutter, B. W., Taylor, S. E., VanBrocklin, H. F., Huesman, R. H., and Budinger, T. F. (2001) Kinetic analysis of $^{125}$I-iodorotenone as a deposited myocardial flow tracer: Comparison with $^{99m}$Tc-Sestamibi. *J. Nucl. Med. 42*, 272−281.
(49) Höglinger, G. U., Féger, J., Prigent, A., Michel, P. P., Parain, K., Champy, P., Ruberg, M., Oertel, W. H., and Hirsch, E. C. (2003) Chronic systemic complex I inhibition induces a hypokinetic multisystem degeneration in rats. *J. Neurochem. 84*, 491−502.
(50) Höglinger, G. U., Carrard, G., Michel, P. P., Medja, F., Lombès, A., Ruberg, M., Friguet, B., and Hirsch, E. C. (2003) Dysfunction of mitochondrial complex I and the proteasome: Interactions between two biochemical deficits in a cellular model of Parkinson's disease. *J. Neurochem. 86*, 1297−1307.
(51) Lannuzel, A., Michel, P. P., Höglinger, G. U., Champy, P., Jousset, A., Medja, F., Lombes, A., Darios, F., Gleye, C., Laurens, A., Hocquemiller, R., Hirsch, E. C., and Ruberg, M. (2003) The mitochondrial complex I inhibitor annonacin is toxic to mesencephalic dopaminergic neurons by impairment of energy metabolism. *Neuroscience 121*, 287−296.
(52) Thiffault, C., Langston, J. W., and Di Monte, D. A. (2000) Increased striatal dopamine turnover following acute administration of rotenone to mice. *Brain Res. 885*, 283−288.

(53) Ilivicky, J., and Casida, J. E. (1969) Uncoupling action of 2,4-dinitrophenols, 2-trifluoromethylbenzimidazoles and certain other pesticide chemicals upon mitochondria from different sources and its relation to toxicity. *Biochem. Pharmacol. 18*, 1389−1401.

(54) Soderlund, D. M., Messeguer, A., and Bowers, W. S. (1980) Precocene II metabolism in insects: Synthesis of potential metabolites and identification of initial in vitro biotransformation products. *J. Agric. Food Chem. 28*, 724−731.

(55) Randriaminahy, M., Witte, L., Kunze, A., Wray, V., and Proksch, P. (1992) Detoxification of naturally occurring chromenes in larvae of the generalist herbivore *Spodoptera littoralis* (Noctuidae). *Biochem. Syst. Ecol. 20*, 711−722.

(56) Škrinjari-Špoljar, M., Matthews, H. B., Engel, J. L., and Casida, J. E. (1971) Response of hepatic microsomal mixed-function oxidases to various types of insecticide chemical synergists administered to mice. *Biochem. Pharmacol. 20*, 1607−1618.

(57) Checkoway, H., Farin, F. M., Costa-Matten, P., Kirchner, S. C., and Costa, L. G. (1998) Genetic polymorphisms in Parkinson's disease. *Neurotoxicology 19*, 635−643.

TX049867R